Available online at www.sciencedirect.com
SCIENCE DIRECT®
Journal of the European Ceramic Society 25 (2005) 817–828
www.elsevier.com/locate/jeurceramsoc

Application of the chemical vapor infiltration and reaction (CVI-R) technique for the preparation of highly porous biomorphic SiC ceramics derived from paper

Daniela Almeida Streitwieser*, Nadja Popovska, Helmut Gerhard, Gerhard Emig

Department of Chemical Reaction Engineering, University Erlangen-Nuremberg Egerlandstrasse 3, D-91058 Erlangen, Germany

Received 30 December 2003; received in revised form 25 March 2004; accepted 3 April 2004
Available online 20 July 2004

Abstract

Chemical vapor infiltration and reaction (CVI-R) is used to produce biomorphic high porous SiC ceramics based on biological structures such as paper. The paper fibers are first converted into a biocarbon (C_b) template by a carbonization step. In a second step methyltrichlorosilane (MTS) in excess of hydrogen is infiltrated into the C_b-template by CVI technique, depositing a Si/SiC layer around each fiber. The reaction (R) between biocarbon and excess silicon to form additional silicon carbide occurs during a subsequent thermal treatment as a third step of the ceramization process. Due to the mild infiltration conditions (850–900 °C) the initial micro- and macrostructure of the carbon preform is retained in the final ceramics. The applied characterization methods after every step of the ceramization process are X-ray Photoelectron Spectroscopy (XPS), Raman spectroscopy, Thermal Gravimetric Analysis (TGA), and Scanning Electron Microscopy (SEM). The bending strength of the resulting porous ceramics is measured by the double ring bending test. It is found that a slight excess of free Si in relation to the amount of carbon from the C_b-template must be deposited in the Si/SiC layer to achieve a nearly complete conversion of the C_b-templates into SiC ceramic. The weight gain after infiltration has to be at least 400 wt.%. Varying the infiltration conditions such as temperature, MTS concentration and infiltration time, ceramics in a wide range of porosity (55–80%) and mechanical properties (5–40 MPa) can be produced. A thermal treatment temperature of 1400 °C is found to be optimal for the reaction between the deposited Si and the biocarbon.

Keywords: Biomorphic ceramics; CVI-R; Fibers; Microstructure; Paper; SiC

1. Introduction

In recent years the characteristics and advantages of natural structures have been recognized and utilized for specific technical applications such as the imitation of natural structures by biomimetic design or as the implementation of biological structures for manufacturing biomorphic ceramics.[1–3] Biomorphic high porous ceramics are obtained by carbonization and consecutive conversion of biological preforms into ceramics. During the conversion the microstructure of the biological preform is neither destroyed nor altered, only a homogeneous shrinkage in all directions takes place during carbonization.[4,5] However, its chemical composition changes due to the ceramization process. The original cellulose molecules of the paper fibers used in this study are first converted into a carbon lattice—the biocarbon (C_b-) template—and then transformed into a SiC ceramic by adding Si to the template and subsequently reacting it with the C_b.[6,7] Additional SiC can be deposited onto the fibers to reinforce the original structure. During this transformation highly specified structures of paper preforms are remained unchanged down to the micrometer level. The ceramics obtained from biological preforms, either paper or wood preforms, show high strength combined with very low density.[7,8]

Up to now it is not possible to produce such high porous ceramic structures using conventional manufacturing technologies.[3,9] For this reason, new methods to produce high porous, light weight ceramics from biological preforms have been developed in the last years.[9] Among these methods the most investigated are Si liquid infiltration,[10–15] Si gas infiltration,[10,16,17] SiO vapor infiltration,[16,18] polymer infiltration[19] and, the method used in this pa-

* Corresponding author. Tel.: +49 9131 852 7437; fax: +49 9131 852 7421.
E-mail address: daniela.almeida@rzmail.uni-erlangen.de (D.A. Streitwieser).

0955-2219/$ – see front matter © 2004 Elsevier Ltd. All rights reserved.
doi:10.1016/j.jeurceramsoc.2004.04.006

per, chemical vapor infiltration and reaction (CVI-R) technique.[6,7,20–23]

Earlier investigations have been performed by Greil et al.[7] on SiC ceramics derived from wood templates to compare three different ceramization methods. In that study the biaxial tensile loading condition perpendicular to the cell elongation has been measured and compared between the SiC ceramics obtained by Si melt infiltration, SiO vapor infiltration and CVI-R technique. The study has shown that the mechanical tensile strength of the CVI-R derived SiC ceramics is almost twice as high as that obtained by Si melt infiltrated samples and over five times higher compared to those obtained from SiO vapor infiltrated samples. For this reason, the CVI-R technique is further developed for the ceramization of C_b-templates derived from papers.

In the present study, paper has been chosen as the preforms for the ceramization of biomorphic materials. Paper preforms have, compared to natural products like wood, the advantage of being an industrial manufactured product, so that the properties of the paper preforms like composition, porosity and density remain constant for different charges due to the reproducible paper manufacturing process. The flat paper sheets can also be formed previous to the processing to any complex three dimensional shape, obtaining thus a high geometric surface area.

The aim of the study is to apply the CVI-R process to convert the porous paper preforms into a ceramic catalyst support. In the first step the paper preforms are converted into a C_b-template by carbonization. During the second step Si/SiC is deposited around each fiber of the C_b-template by CVI. This is followed by a thermal treatment as the last step of the ceramization process, where a solid–solid reaction between the excess Si from the deposited Si/SiC layer and the carbon from the template takes place. In Fig. 1, an overall flow chart of the ceramization process with the CVI-R technique used in this study is presented.

In this paper, each of the three steps in the ceramization process is investigated, with a special focus on the influence of the infiltration conditions of the CVI step on the properties of the resulting biomorphic ceramics. An isothermal and isobaric chemical vapor infiltration (ICVI) process at low temperatures has been applied for the infiltration using methyltrichlorosilane (MTS—CH_3SiCl_3) in excess of hydrogen as precursors. Under these conditions the deposits consists of SiC with an excess of Si. This layer composition is favorable for the formation of biomorphic ceramics from C_b-templates, since the Si reacts during the subsequent thermal treatment by a solid–solid reaction with the biocarbon from the template to SiC, whereas the codeposited SiC reinforces the structure in the micrometer level. By varying the infiltration conditions, the composition of the deposit and the layer thickness, it is possible to control the porosity and thus the mechanical properties of the final ceramics. The main interest of the present study is to find out at which infiltration conditions porous ceramics with high mechanical strength can be obtained.

2. Experimental techniques

2.1. Ceramization steps

2.1.1. Carbonization

The substrates used in this study are flat paper preforms of 0.8 mm thickness with a geometrical density of 0.22 g/cm^3. The initial porosity of the papers is 82% with a mean pore size of 25 μm. Considering the shrinkage in the structures during the processing, the papers are cut to 40 mm × 40 mm squares and carbonized at the conditions described below.

The first step in the ceramization process is the carbonization of the paper preforms. For the carbonization a tubular alumina reactor heated in a resistance furnace is used. To obtain flat samples the paper sheets must be placed in the reactor between two metallic plates, so that they cannot deform during the carbonization process. The samples are first heated with a slow heating ramp of 1 K/min up to 350 °C and kept constant for 1 h. On a second ramp the samples are heated with 2 K/min up to 850 °C and kept at this temperature for another hour, before cooling down to room temperature with 2 K/min. The obtained C_b-templates are used as preforms for the following infiltration process.

2.1.2. Chemical vapor infiltration (CVI)

The experimental equipment used for the CVI step is a conventional tubular hot wall reactor consisting of an alumina tube with 32 mm inner diameter and 0.9 m length. The gases, hydrogen and helium, are dosed by mass flow controllers. The liquid precursor MTS is brought into the gas phase before entering the reactor by bubbling a carrier gas through an evaporator. Based on the vapor pressure curve the desired amount of MTS in the gas phase can be dosed exactly by setting the evaporator temperature. A flow chart of the CVD/CVI equipment is presented in Fig. 2. The inner reactor wall is lined with a graphite foil in order to be able to consider the codeposition on the reactor wall[26] and to protect the alumina tube. The substrates, C_b-templates, are positioned at the beginning of the isothermal zone, where a homogeneous deposition rate is observed. The investigated parameter scope is limited to the low temperature region between 850 and 900 °C. The infiltration is carried out at

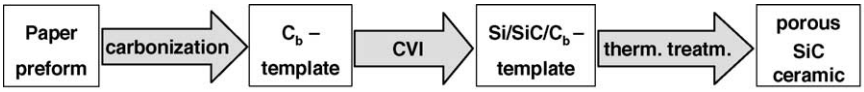

Fig. 1. Flow chart of the ceramization process by CVI-R technique.

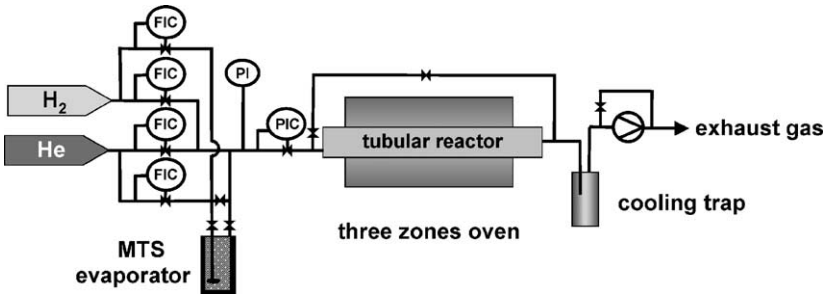

Fig. 2. Flow chart of the CVI equipment.

atmospheric pressure. The MTS concentration is varied from a low molar fraction of 0.01 to a high molar fraction of 0.10 and the corresponding hydrogen to MTS ratio α ranged from 9 to 90. At this deposition conditions the films consist of Si-rich SiC deposits.

To define the surface reaction limited regime and to determine the composition of the deposits as function of the infiltration parameters, preliminary CVD investigations on nonporous graphite substrates are performed. For these investigations graphite samples, consisting of 30 graphite foil strips bent to semicircles, are placed along the whole length of the reactor in order to determine the axial deposition rate profiles and to analyze the composition of the deposits as function of the infiltration parameters.[26]

2.1.3. Thermal treatment (reaction)

The last step in the ceramization process is the chemical reaction between the Si from the Si/SiC deposit and the C from the C_b-template. This reaction takes place in the solid phase and has to be performed at elevated temperatures. For this study the temperature is varied between 1250 and 1600 °C. The thermal treatment time is kept constant at 1 h. The effect of the thermal treatment conditions on the solid–solid reaction is evaluated by the content of unreacted Si and residual carbon, measured by Raman spectroscopy and Thermo Gravimetric Analysis (TGA), respectively.

2.2. Characterization methods

The composition of the deposits is determined by X-ray photoelectron spectroscopy (XPS, Physical Electronics PHI 5600 ESCA System). XPS is performed on the nonporous samples to obtain the atomic composition of the deposited films prior to its reaction with the carbon from the template.

Raman spectroscopy (Raman-Spektrometer Type Renishaw Ramascope 2000) is used to analyze the molecular composition of the ceramics (C, Si, SiC) on the fibers surface after every step in the ceramization process. In this method the molecular vibrations are measured in the form of scattered Raman radiations generated by a monochromatic laser beam ($\lambda = 514$ nm). The scattered light is disjointed according to the wavelength and then recorded in the detector, so as to recognize different atoms and functional groups.

TGA (Simultan-Thermo-Analyse-Geraet STA 429 Firma Netzsch-Gerätebau GmbH) is used to obtain the mass change of a sample while being submitted to a specified temperature-time-program. For this study, the residual carbon in the final ceramics is being detected by TGA since it oxidizes easily in air at temperatures above 400 °C. Therefore, the mass loss of the samples oxidized at 750 °C for 4 h in air flow (30 Nl/h) is proportional to the amount of unreacted carbon in the ceramic.

Scanning Electron Microscopy (SEM, Phillips XL 30) is a useful technique for analyzing the surface morphology of the preforms at every processing step. With this method it is possible to see the changes in the samples after each step and for the different process conditions.

The porosity of the samples after each processing step is determined by Mercury (Hg-) porosimetry. It is based on the high surface tension property of mercury. When performing the pore size measurement, mercury has to be forced into the porous specimen with the pressure increased in steps. The amount of mercury intruded is determined and pore size, pore size distribution and porosity are obtained.[23] In this study, Carlo Erba Mercury Intrusion Porosimeter 2000 is applied.[24] The results are compared to the values obtained from calculations using the geometrical and the strut density of the samples.

Finally, in order to be able to make a statement about the quality of the processed ceramics, the bending strength is determined by a double ring bending test according to DIN 52 292[25] for flat samples of glasses and glass ceramics. The samples are subjected to a bending strength in radial and tangential direction between two metallic rings. A scheme of the double ring bending test arrangement is shown in Fig. 3. The bending strength of a sample, $\sigma_{b,max}$, is the tensile strength reached at the first crack of the sample. It

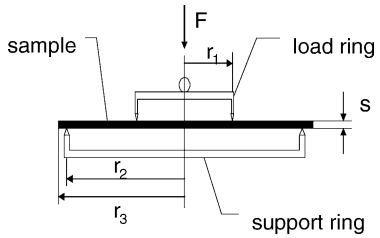

Fig. 3. Scheme of the double ring bending test arrangement.

can be calculated from the maximal load, $F_{max'}$ and the thickness of the sample, s.

$$\sigma_{b,max} = 1.04\frac{F_{max}}{s^2} \quad (1)$$

By this method, only a spherical area of the sample as big as the support ring is submitted to the force, but not the margins of it.

3. Results and discussion

3.1. Carbonization

The carbonization reactions of natural fibers have been extensively studied in earlier papers.[4,10,13,17] Basically the paper preforms consisting of cellulose are exposed to a high temperature treatment in inert atmosphere. In the first heating ramp, up to 350 °C, volatile species like H_2O, CO, CO_2, aliphatic acids, carbonyls, and alcohols are released from the substrates.[13] The major mass loss is observed between 220 and 350 °C. In the second heating ramp, at high temperatures polyaromatic carbon compounds are formed. They can be either transported out of the reactor by the gas phase as high viscous bitumen-like by-products or they react further to form the carbon lattice structure.

The mass loss of the paper preforms after carbonization is about 80 wt.%. Shrinkage in all directions is also observed. The macroscopic shrinkage in length and height is 26% and lies somewhat higher in width with 33% due to the paper manufacturing process, where the fibers obtain a certain orientation. For the same reason the thin paper sheets tend to bend and roll during the carbonization. To obtain flat samples they must be weighted down with a flat heat resistant support during the process.

The geometrical density of the resulting C_b-templates is 0.125 g/cm^3 with a porosity of 90%. In Fig. 4, SEM micrographs of a paper (Fig. 4a) and a C_b-template (Fig. 4b) are shown. Each fiber retains its initial structure with shrinkage in diameter between 25 and 33%.

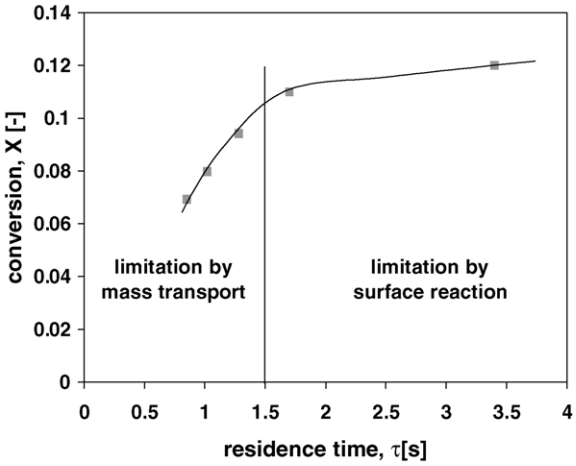

Fig. 5. Dependence of the precursor conversion on the residence time.

3.2. Chemical vapor infiltration

3.2.1. Preliminary investigations—CVD on nonporous substrates

Preliminary investigations have to be performed on nonporous substrates prior to the infiltration experiments in order to define a region of deposition conditions where no mass transport limitations take place and where the surface reaction controls the overall deposition process. This means, that in this region the rate of mass transport of the reactants to the substrate surface is higher than the deposition reaction on the surface. Only under such conditions a homogeneous infiltration in the preforms can be obtained.

Generally, mass transport limitation by film diffusion or convection can easily be verified by varying the residence time of the gases, expressed as the gas flow velocity, keeping other reaction conditions constant. The surface reac-

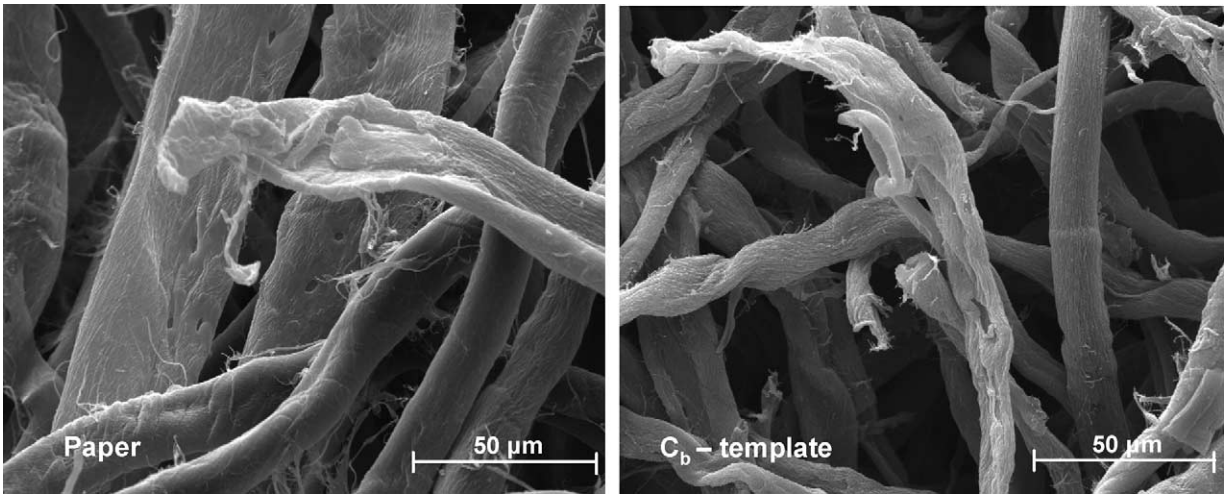

Fig. 4. SEM micrograph of the structure of the (a) paper and (b) C_b-template.

tion limited regime lies at a residence time region where a maximum conversion of the precursor is observed. Fig. 5 shows the influence of the residence time of the reactant gases on the conversion of the precursor MTS. It can be seen that at residence times smaller than 1.5 s the conversion increases with the residence time, which indicates that the deposition process is limited by mass transport. By increasing the residence time above 1.5 s the conversion achieves a maximum value remaining constant independent from the residence time, which indicates that in this region the deposition process is limited by the surface reaction. Therefore, a residence time of 1.5 s, corresponding to a gas flow velocity of 30 cm/s, is assumed to be optimal for the following experiments, in order to achieve a homogeneous infiltration into the pores of the C_b-template.

Furthermore, the composition of the deposited films as a function of temperature and hydrogen excess has been analyzed on nonporous graphite substrates by XPS. A detailed decomposition mechanism of methyltrichlorosilane and hydrogen to SiC, Si/SiC, and C/SiC is postulated by Popovska et al.[26] in a previous study. Though, for better understanding a simplified overall deposition reaction of Si/SiC is presented in Eq. (2).

$$(x+y)CH_3SiCl_3 \xrightarrow{H_2} xSi(s) + ySiC(s) + xCH_4 + 3(x+y)HCl \quad (2)$$

The composition of the deposits expressed as the Si/C ratio depends on both deposition temperature and hydrogen amount in the reaction gas as shown in Fig. 6.

It is found that at the chosen infiltration conditions: low temperature region between 850 and 900 °C and high hydrogen excess, the deposited layers surrounding the carbon fibers of the C_b-template have a Si to C ratio of 2.5–3.5, corresponding to a Si/SiC ratio of 1.5–2.5.

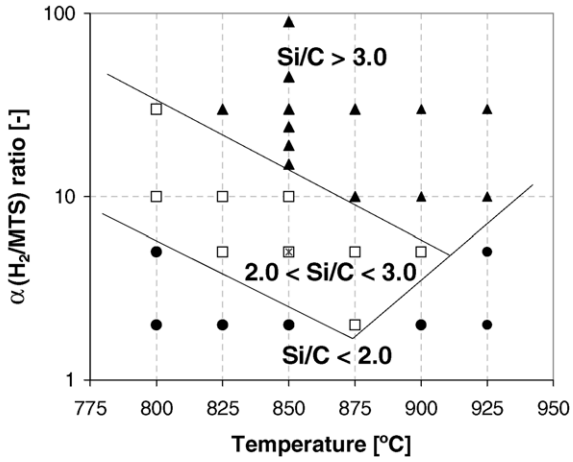

Fig. 6. Analysis of the layer composition as function of temperature and hydrogen excess.

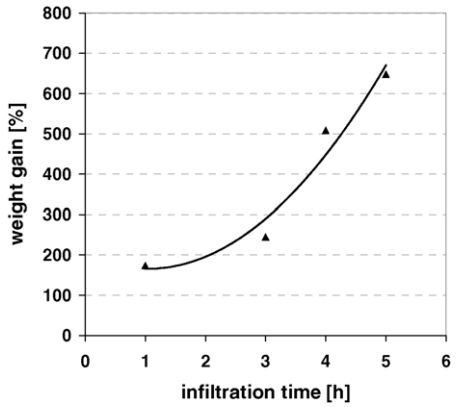

Fig. 7. Influence of the infiltration time on the weight gain of the C_b-templates ($T = 850$ °C).

3.2.2. *Chemical vapor infiltration of the C_b-templates*

The chemical vapor infiltration of the C_b-templates prepared by carbonization of paper has been studied by performing different series of experiments. The infiltration parameters with the major influence on the properties of the resulting ceramics such as temperature, MTS molar fraction and infiltration time have been investigated independently from each other. The dependence of the infiltrated layer thickness, expressed as percent weight gain of the C_b-templates, on the infiltration time at MTS molar fractions of 0.05 and 850 °C is shown in Fig. 7. As it can be seen, the weight gain rises as a second order function with the infiltration time.

After having analyzed the influence of the infiltration time, the following experiments with variation of temperature and MTS molar fraction are done with 1-h infiltration. Fig. 8 shows the combined effect of the variation of the infiltration temperature from 850 to 900 °C and the MTS molar fraction from 0.01 to 0.10 using a maximum amount of hydrogen ($\alpha = H_2/MTS = 99–9$). The deposition rate increases linearly with the MTS molar fraction for all temperatures investigated. At 850 and 900 °C the weight gain rises by a factor of 2 when the molar fraction is doubled

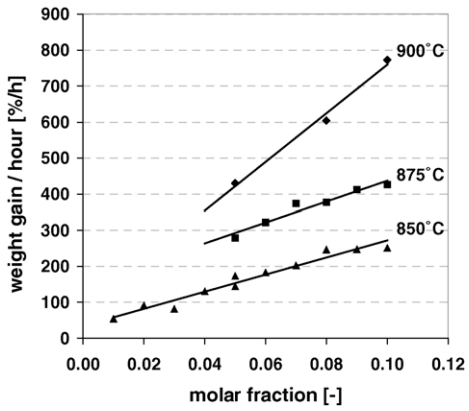

Fig. 8. Influence of the MTS molar fraction and the infiltration temperature weight gain of the C_b-templates.

from 0.05 to 0.10. Generally, it can be concluded that a temperature rise of 25 °C doubles the deposition rate and has thus the same effect as doubling the MTS molar fraction. The infiltration conditions affect strongly the properties of the final ceramics as described below.

3.2.3. Effect of the infiltration conditions on the properties of the resulting ceramics

In order to investigate the effect of the infiltration conditions on the properties of the resulting ceramics, all the samples have been thermally treated at the same conditions (1 h at 1400 °C) after infiltration.

3.2.3.1. Composition of the ceramics. After the ceramization process, the ceramics may consist of residual C from the template, unreacted Si and deposited as well as thermally reacted SiC. In the preliminary investigations (see Section 3.2.1) the composition of the deposited layers around the carbon fibers of the C_b-template at different infiltration conditions are determined. In Table 1 the deposited masses of free Si and SiC and the corresponding molar ratio between the free Si and the C_b from the template, n_{Si}/n_{C_b}, are listed. The n_{Si}/n_{C_b} ratio increases with increasing MTS molar fraction and temperature, since these parameters increase the deposition rate and therefore the weight gain and the overall moles of Si that can react with the C_b. A weight gain of at least 400 wt.% is needed to reach the amounts of Si necessary for stoichiometric reaction with C_b to SiC.

The effect of the infiltration conditions on the composition of the resulting ceramics is also analyzed by Raman spectroscopy and TGA. Fig. 9 shows the Raman spectra of the C_b-templates infiltrated for 1 up to 5 h at 850 °C and at 0.05 MTS molar fraction. Already after 3-h infiltration no more carbon is found on the surface. For 1- and 3-h infiltration time, no Si peak can be observed, indicating a complete

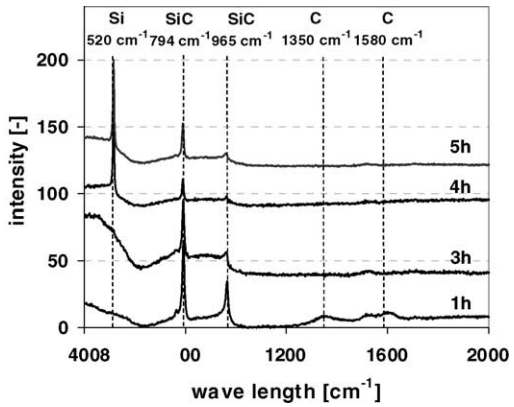

Fig. 9. Raman spectra of the ceramized samples infiltrated for different infiltration time.

reaction of Si with the C_b to SiC. For 4- and 5-h infiltration time, a sharp Si peak appears since not all the Si can diffuse through the thick deposited layers in order to react with the carbon core. Fig. 10 shows the Raman spectra of the C_b-templates infiltrated at 850 °C (Fig. 10a) and 900 °C (Fig. 10b). Residual carbon is detected at all MTS molar fraction values at 850 °C infiltration temperature. As shown in Fig. 8 the maximum weight gain under these conditions is 252 wt.% and a n_{Si}/n_{C_b} ratio below 0.56 is calculated in Table 1. This explains why residual carbon is still observed on the fiber surfaces. The amount of the free Si in the Si/SiC deposit has not been enough to convert the C_b-template completely into a SiC ceramic. At 900 °C no carbon peaks are detected by Raman spectroscopy. The calculated n_{Si}/n_{C_b} ratio lies between 1.1 and 1.9 with a weight gain between 430 and 780 wt.%. The Si peak is still observed at all MTS molar fractions. For the MTS molar fraction of 0.10 no sharp SiC peak is observed. The Si is found to be the major species on the surface.

Table 1
Compositional analysis of the deposited layers

Infiltration parameters			Initial mass of C_b, m_{C_b} (g)	Total mass gain, Δm (%)	Si/SiC deposit		Moles free Si, n_{Si}	Moles C_b, n_{C_b}	Ratio n_{Si}/n_{C_b}
T (°C)	X_{MTS}	α			Mass of free Si (g)	Mass of SiC (g)			
850	0.05	19	0.05474	173	0.0554	0.0395	0.0020	0.0046	0.4325
850	0.06	15	0.06290	183	0.0672	0.0480	0.0024	0.0052	0.4569
850	0.07	13	0.06121	203	0.0726	0.0518	0.0026	0.0051	0.5071
850	0.08	11	0.05881	246	0.0749	0.0699	0.0027	0.0049	0.5449
850	0.09	10	0.05734	248	0.0735	0.0686	0.0026	0.0048	0.5481
850	0.1	8.5	0.05736	252	0.0747	0.0697	0.0027	0.0048	0.5570
875	0.05	19	0.06040	279	0.0982	0.0701	0.0035	0.0050	0.6956
875	0.06	15	0.06224	322	0.1170	0.0835	0.0042	0.0052	0.8039
875	0.07	13	0.05941	375	0.1301	0.0929	0.0046	0.0049	0.9367
875	0.08	11	0.06250	377	0.1375	0.0981	0.0049	0.0052	0.9408
875	0.1	9	0.05753	426	0.1429	0.1020	0.0051	0.0048	1.0622
875	0.09	10	0.05846	412	0.1405	0.1003	0.0050	0.0049	1.0277
900	0.05	19	0.01712	430	0.0430	0.0307	0.0015	0.0014	1.0736
900	0.07	13	0.01874	604	0.2038	0.1455	0.0073	0.0048	1.5067
900	0.08	11	0.05786	779	0.0852	0.0608	0.0030	0.0016	1.9438
900	0.1	9	0.05202	773	0.2345	0.1674	0.0083	0.0043	1.9279

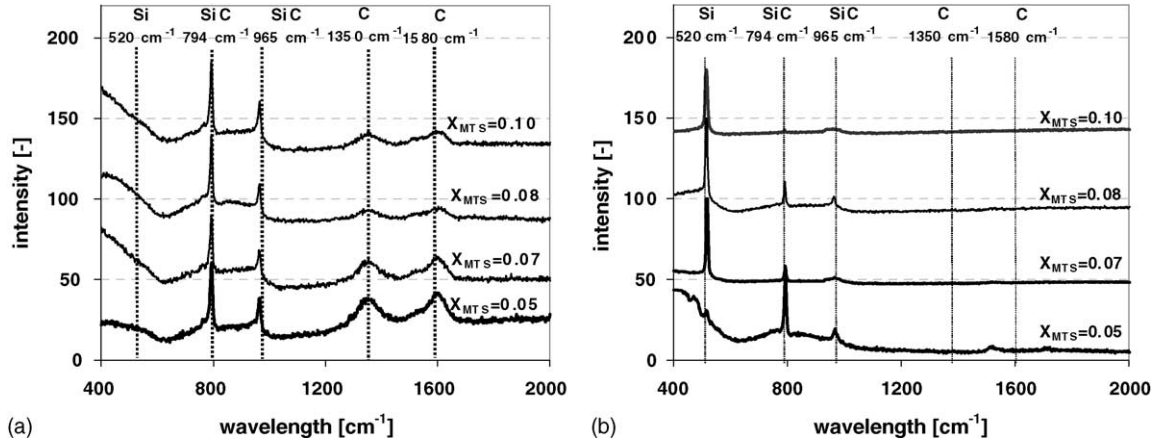

Fig. 10. Raman spectra of the ceramized samples infiltrated at (a) 850 °C and (b) at 900 °C.

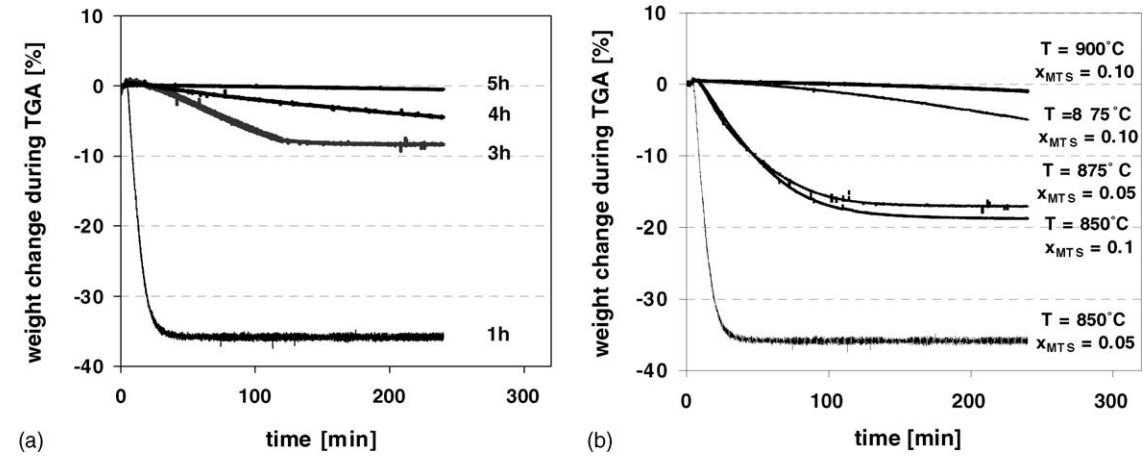

Fig. 11. TGA of the ceramics infiltrated at different conditions: (a) variation of the infiltration time and (b) variation of the temperature and MTS molar fraction.

The degree of conversion of carbon to SiC ceramic at different infiltration conditions is also analyzed by TGA, expressed as a weight change after isothermal treatment at 750 °C in air flow, where the residual C is oxidized (Fig. 11). In Fig. 11a, the weight change for variation of the infiltration time is presented. It can be seen that the degree of conversion and the weight gain are proportional to the infiltration time. The sample at 1 h infiltration has a weight gain of only 180 wt.% and a n_{Si}/n_{C_b} ratio of 0.43 and shows a weight loss over 35 wt.%. At higher infiltration times, the weight loss lies in the range between 5 wt.% and almost no mass loss after 5 h infiltration. The same tendency is observed with an increase of the MTS molar fraction and the temperature in Fig. 11b. Though, the temperature has a much higher influence. At 900 °C and MTS molar fraction of 0.10 nearly no mass loss is observed in TGA, indicating a complete conversion of the C_b into SiC.

Fig. 12 shows the relationship between the n_{Si}/n_{C_b} ratio in the ceramics after infiltration and the obtained weight change during TGA. A complete conversion of the C_b into SiC occurs only if the n_{Si}/n_{C_b} ratio exceeds 1.0, corresponding to a weight gain of at least 385 wt.%. At a n_{Si}/n_{C_b} ratio of 1.2 almost complete conversion is achieved.

3.2.3.2. Morphology of the ceramics. The primary goal of this study is to process stable, high porous SiC ceramics retaining the initial microstructure of the paper fibers. SEM is used to study the morphology of the samples after each processing step. The conversion of the C_b-template to SiC and

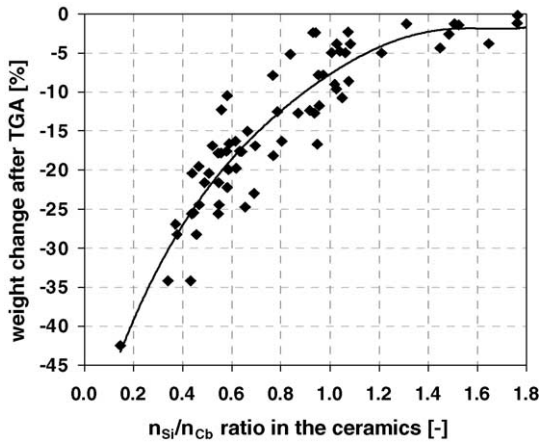

Fig. 12. Relationship between the Si/C ratio in the ceramics and the weight change by TGA.

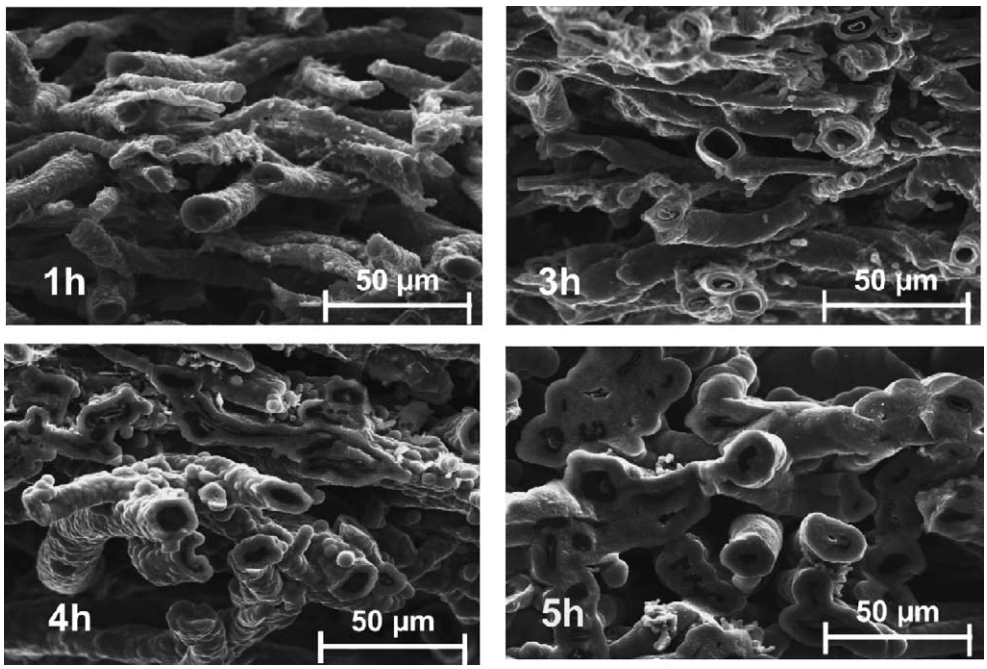

Fig. 13. SEM micrograph of the infiltrated ceramics at 1, 3, 4, and 5 h ($T = 850\,^{\circ}C$, $X_{MTS} = 0.05$).

the reinforcement by additional deposited SiC can be clearly seen from the SEM micrographs. In Fig. 13 the SEM micrographs of the samples infiltrated for different times at 850 °C and 0.05 MTS molar fraction are presented. The sample with 1 h infiltration time has only a few nanometer thin layer of SiC deposited around each fiber. The corresponding weight gain lies below 200 wt.%. For 3 and 4 h infiltration the fiber structure is retained to a high extend with much thicker layers between 2 and 4 μm and a weight gain between 250 and 500 wt.%. After 5 h infiltration, the fibers stick together and form clusters of coated fibers. The layer thickness is around 6 μm. This sample has a weight gain of above 600 wt.%.

For the experiment series with variation of the infiltration temperature, only the samples infiltrated at a MTS molar fraction of 0.10 are presented in Fig. 14. Around each fiber a thick SiC layer has been deposited and some have grown together with the adjacent fibers. The mean SiC layer thickness for 850, 875, and 900 °C lies at 2, 3, and 6 μm, respectively. The carbon core is still present in all the samples, though at 900 °C it is very small.

It can be concluded that at weight gains up to 400 wt.% the original microstructure of the C_b-template is retained to a high degree, while at higher weight gains the structure is modified by the formation of SiC clusters and increase in the thickness of the individual fibers. The porosity of the samples also decreases due to this increase in material, filling the void between the fibers.

3.2.3.3. Mechanical properties. All the ceramics have been submitted to double ring bending test to obtain a value for its bending strength. From the results it can be seen that the maximal bending strength is only a function of the final porosity of the ceramics. The porosity is linearly related to the weight gain and can be calculated from the geometrical density and measured by Hg-porosimetry. No difference can be observed in samples with similar weight gain but obtained under different infiltration conditions.

The geometrical density of the ceramics lies in the range between 0.3 and 1.3 g/cm^3 and it increases linearly with the weight gain after infiltration as shown in Fig. 15. For low weight gains below 200 wt.% no significant difference can be observed compared to the C_b-template. But for the highest value of 800 wt.%, the geometrical density increases to a maximum value of 1.3 g/cm^3. Assuming that the ceramic consists only of SiC with a density of 3.22 g/cm^3 the open porosity of the ceramics can be calculated. The porosity is inversely proportional to the weight gain and it changes from very high values around 80% to a moderate porosity of 55%.

Fig. 16 shows the dependence between the maximal bending strength of the ceramics and their final porosity after the ceramization process. The bending strength remains almost constant at values between 5 and 10 MPa for high porous samples with porosity between 70 and 80%, increasing rapidly with decreasing the porosity to values below 70%. This behavior can be confirmed by the SEM micrographs, where high porous samples are obtained at low weight gains between 200 and 400 wt.%. The properties of the C_b-template dominate the overall structure. At higher weight gains, the porosity decreases linearly with the amount of deposited material since the deposited Si/SiC reinforces the original structure. The values for the maximal strength for ceramics with a weight gain of 800 wt.% and a corresponding porosity of 55% lies above 40 MPa. This value is extremely high for porous ceramics compared to ceramics manufactured by any other technique.[7]

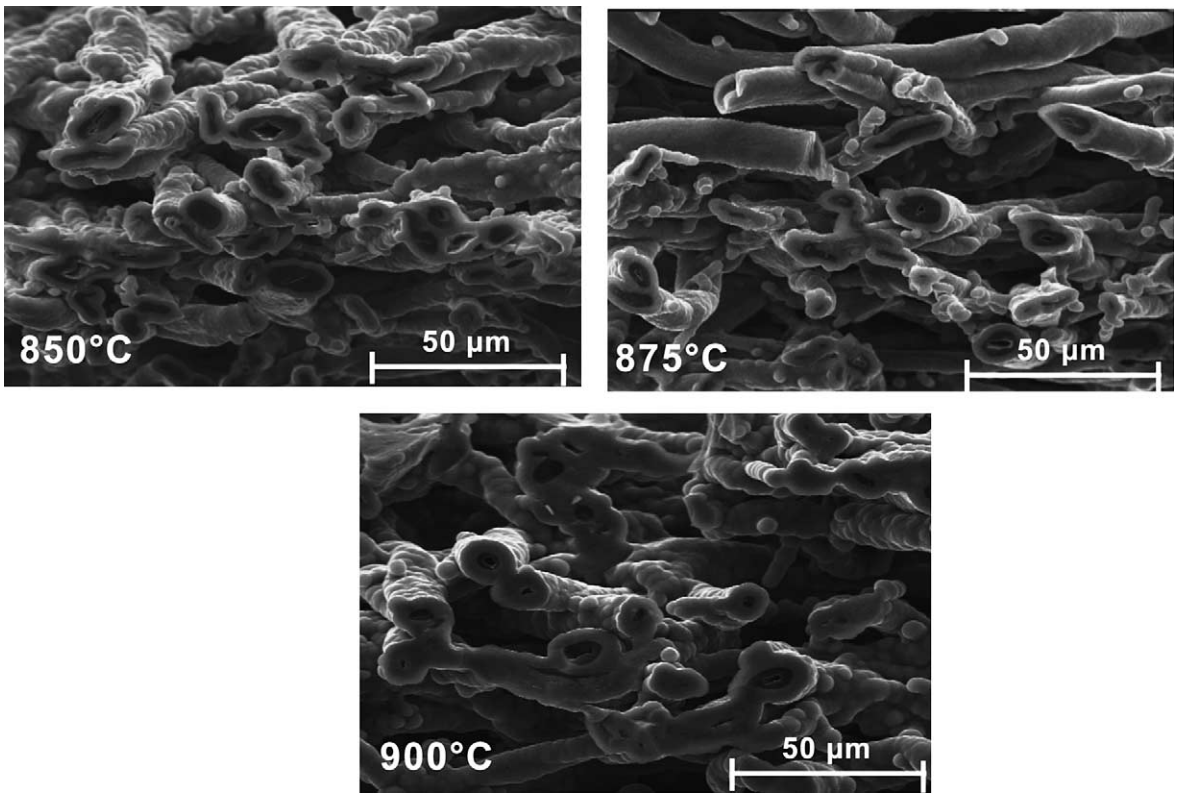

Fig. 14. SEM micrograph of the infiltrated ceramics at 850, 875, and 900 °C at an MTS molar fraction of 0.1.

Ceramics in a wide range of porosity and mechanical strength can be obtained adjusting the infiltration conditions. The regime lies between denser materials with a porosity of 55% and a bending strength up to 40 MPa and light ceramics with a high porosity of 80–65% and a bending strength of 10–20 MPa. The dense ceramics are produced by infiltration at 900 °C and MTS molar fraction of 0.10 or at longer infiltration times above 4 h at 850 °C. The light ceramics can be produced by an infiltration of 1 h at 875 °C and MTS molar fraction of 0.08–0.10 or at 900 °C and low MTS molar fraction of 0.05. The infiltration regimes can be varied depending on the desired characteristics of the resulting ceramics. If the ceramics should to be applied as catalysts supports at high temperatures in oxidizing atmospheres, the residual carbon must be burnt out before its application.

3.3. Thermal treatment (reaction)

3.3.1. Solid–solid reaction

During the infiltration step amorphous SiC coatings with excess of Si are deposited around the carbon fibers of the

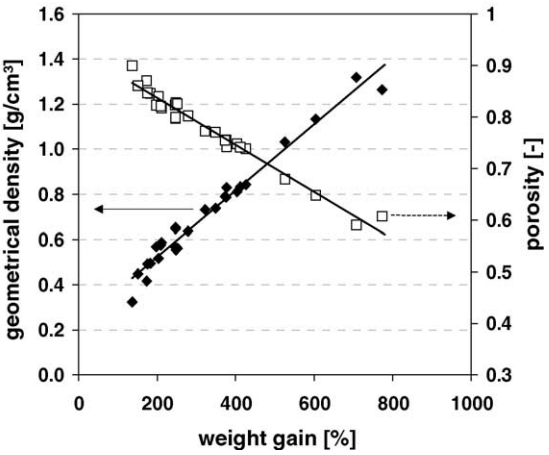

Fig. 15. Influence of the weight gain after infiltration on the geometrical density and the porosity of the obtained ceramics.

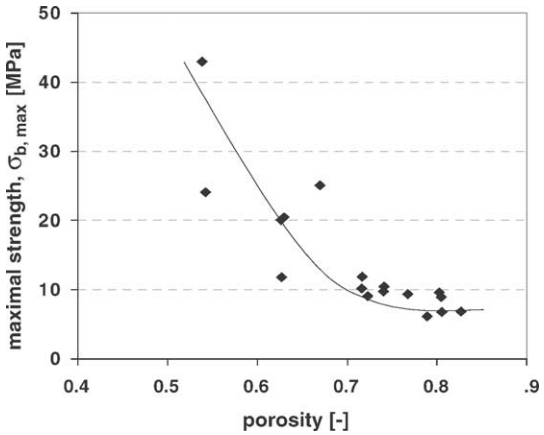

Fig. 16. Maximal strength of the ceramics, as a function of the porosity of the final ceramics.

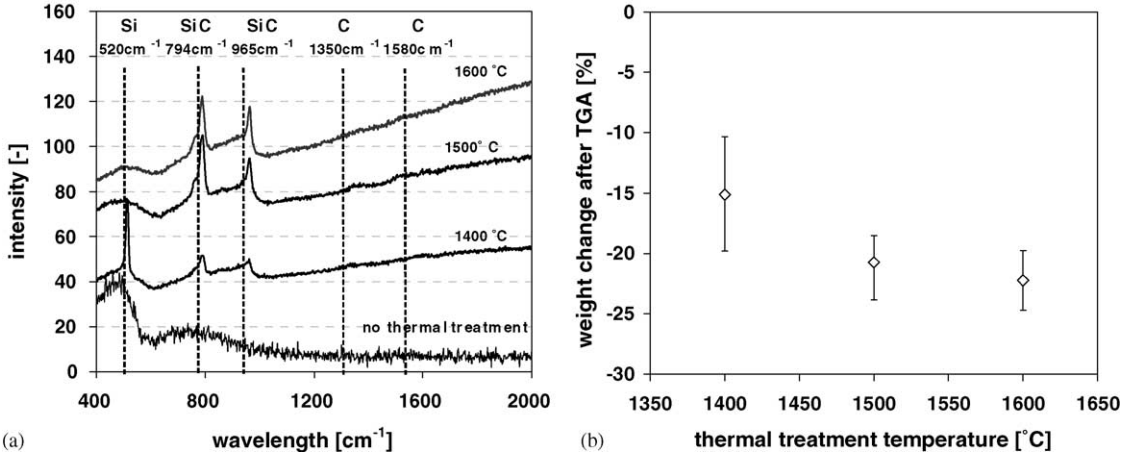

Fig. 17. Effect of the temperature of the thermal treatment on the conversion of the C_b analyzed by (a) Raman spectroscopy and (b) TGA.

C_b-template. By a following thermal treatment the excess Si reacts with the carbon from the C_b-template to form crystalline SiC. The difference between the amorphous and the crystalline SiC can be seen in the width of the Raman peaks as shown in Fig. 17. This solid–solid reaction is limited by the rate of solid phase diffusion of the Si and the carbon through the already formed SiC layer.[27] The diffusion coefficient increases with the temperature until approaching the melting point of the species. The melting point of Si is 1420 °C. So at temperatures below 1420 °C the Si will diffuse in the solid phase through the imperfections of the crystalline SiC layer. For temperatures above 1420 °C, melted Si can evaporate and diffuse as a liquid or a gas into the carbon core at the fibers center or it can also diffuse out of the sample.

Kanino et al.[28] observed in High Resolution Electron Microscopy that Si atoms diffuse through SiC, react with carbon and form SiC crystals at about 1400 °C. The diffusion coefficient of Si in single crystalline SiC is negligible small, so the possibility for Si to diffuse through the growing SiC layer is directly proportional to the structural and morphological imperfections in the layer.[29] Cimalla et al.[29] calculated a value of 4.0×10^{-13} cm^2/s at 1250 °C obtained for CVD grown layers of a few micrometers. Using an Arrhenius dependence of the diffusion coefficient on the temperature, the diffusion coefficient at 1400 °C is calculated to 6.0×10^{-13} cm^2/s. This value is still too small to obtain acceptable rates of diffusion.[27] Investigations have been done at temperatures below 1400 °C, but no reaction between Si and carbon can be observed because of the low diffusion coefficients. Therefore, the minimum temperature for the thermal treatment is set to 1400 °C. At higher temperatures the melting point of Si is reached, which may cause the unreacted Si to melt or to evaporate through morphological imperfections of the SiC to the carbon core or out of the sample. Probably a part of the Si diffuses to the inner core of the carbon, but some Si nearer to the outer surface evaporates out of the sample. For this reason, as already shown, unreacted carbon is still found after TGA when stoichiometric and over-stoichiometric amounts of free Si, $n_{Si}/n_{C_b} \geq 1$, have been deposited on the samples.

3.3.2. *Effect of the thermal treatment conditions on the properties of the resulting ceramics*

In order to investigate the effect of the thermal treatment conditions, the infiltration parameter are kept constant at 850 °C, 0.05 molar fraction of MTS and 3-h infiltration time. The composition of the resulting ceramics at different thermal treatments is analyzed by Raman spectroscopy. The intensity of the peaks increases with the crystallinity of the phases. Since the infiltrated layers are amorphous before the thermal treatment, no peak can be detected after infiltration as shown in Fig. 17a. After a thermal treatment at 1400 °C SiC turns crystalline and Si can still be found on the sample surface, but after a thermal treatment at 1500 and 1600 °C only SiC is observed.

This result indicates that Si has either diffused through the layer reacting completely to SiC or it has melted and evaporated out of the sample. To analyze the residual carbon in the inner core the ceramics are exposed to TGA isothermally at 750 °C in air flow. The weight loss due to the oxidation of the carbon is shown in Fig. 17b. For similar Si/C ratios the weight change increases at higher temperatures of the thermal treatment due to evaporation of liquid Si out of the sample instead of its diffusion through the SiC layer and reaction with C_b. Therefore, there is no benefit from thermal treatment temperatures above 1400 °C.

In Table 1 the ratio of infiltrated free Si to C_b from the template, n_{Si}/n_{C_b}, is presented for different infiltration conditions. The amount of unreacted carbon is determined by TGA. The weight loss obtained by TGA increases at low n_{Si}/n_{C_b} ratios linearly, but at higher n_{Si}/n_{C_b} ratios above unity, a stagnation in the weight loss is observed at 5–2% as shown in Fig. 12. These results indicate that at a thermal treatment of 1 h at 1400 °C no complete conversion to SiC is achieved even if overstoichiometric amounts of free Si, $n_{Si}/n_{C_b} \geq 1.2$, are available. The calculated diffusion distance after 1-h thermal treatment is only

0.66 μm.[27] For that reason a longer treatment time should be applied.

4. Conclusions

The ceramization of paper fibers by a three-step process consisting of carbonization, chemical vapor infiltration and solid–solid reaction during a thermal treatment has been investigated.

After the carbonization step the obtained biocarbon (C_b-) templates retain its exact microstructure. The consecutive chemical vapor infiltration and reaction steps convert the C_b-templates into ceramics with properties varying in a wide range.

It is found that for a higher degree of conversion of carbon into SiC ceramic a n_{Si}/n_{C_b} ratio after infiltration higher than 1.2 and a weight gain of at least 400 wt.% is necessary. From the SEM micrographs it can be seen that the fibers grow together when the weight gain is around 800 wt.%.

The geometrical density of the SiC ceramics is proportional and the porosity is reverse proportional to the weight gain. This shows a clear dependence of the properties of the ceramics on the infiltration conditions. The bending strength of the ceramics with its 5–10 MPa is almost independent of the weight gain in a region between 200 and 400 wt.%, where porosity between 70 and 80% of the samples is observed. At lower porosities the strength increases rapidly to the obtained maximum value of 42 MPa at 55% porosity.

The thermal treatment at temperature above 1400 °C shows no benefit in the conversion of carbon to SiC as no more Si has diffused and reacted with the carbon, but rather it has evaporated out of the sample.

Acknowledgements

The authors thank the German Ministry of Education and Research (BMBF) for the financial support as part of the program: Development of Biomorphic Ceramics for the Exhaust Gas Treatment (03N8018E).

References

1. Greil, P., Lifka, T. and Kaindl, A., Biomorphic cellular silicon carbide ceramics from wood: I. Processing and microstructure. *J. Eur. Ceram. Soc.* 1998, **18**, 1961–1973.
2. Calvert, P. and Rieke, P., Biomimetic mineralization in and on polymers. *Chem. Mater.* 1996, **8**, 1715–1727.
3. Ahmad, Z. and Mark, J. E., Biomimetic materials: recent developments in organic–inorganic hybrids. *Mater. Sci. Eng.* 1998, **C 6**, 183–196.
4. Hoffmann, C., Kaindl, A., Sieber, H. and Greil, P., *Biomorphe Verbundkeramiken mit zellularen Mikrostrukturen, Verbundwerkstoffe und Werkstoffkunde*. DGM/WILEY-VCH, 1999, pp. 393–398.
5. Sieber, H. and Greil, P., *Herstellung strukturierter Verbundkeramiken aus biologischen Vorformen, Verbundwerkstoffe und Werkstoffkunde*. DGM/WILEY-VCH, 1999, pp. 307–312.
6. Sieber, H., Vogli, E., Müller, F., Greil, P., Popovska, N. and Gerhard, H., CVI-R gas phase processing of porous biomorphic SiC-ceramics. *Key Eng. Mater.* 2001, **206–213**, 2013–2016.
7. Greil, P., Vogli, E., Fey, T., Bezold, A., Popovska, N., Gerhard, H. and Sieber, H., Effect of microstructure on the fracture of biomorphous silicon carbide ceramics. *J. Eur. Ceram. Soc.* 2002, **22**, 2697–2707.
8. Greil, P., Lifka, T. and Kaindl, A., Biomorphic cellular silicon carbide ceramics from wood: II. Mechanical properties. *J. Eur. Ceram. Soc.* 1998, **18**, 1975–1983.
9. Zhou, B., Biomimetic design and test of composite materials. *J. Mater. Sci. Technol.* 1993, **9**, 9–19.
10. Sieber, H., Hoffmann, C., Kaindl, A. and Greil, P., Biomorphic cellular ceramics. *Adv. Eng. Mater.* 2000, **2**(3), 105–109.
11. Sieber, H., Kaindl, A., Schwarze, D., Werner, J.-P. and Greil, P., Light weight cellular ceramics from biologically-derived preforms. *cfi/Ber. DKG* 2000, **77**(1/2), 21–24.
12. Varela-Feria, F. M., López-Robeldo, M.J., Martínez-Fernández, J. and Arellano-López, A.R., Precursor selection for property optimization in biomorphic SiC ceramics. *Ceram. Eng. Sci. Proc.* 2002, **23**(4), 681–687.
13. Herzog, A., Vogt, U., Graule, T., Zimmermann, T. and Sell, J., Characterization of the pore structure of biomorphic cellular silicon carbide derived from wood by mercury porosimetry, Ceramic Materials and Components for Engines. In *Seventh International Symposium*. Goslar, Germany, 2001, pp. 505–512.
14. Varela-Feria, F. M., De Arellano-Lobredo, A. R. and Martínez-Fernández, J., Fabricación y Propiedades del Carburo de Silicio Biomórfico: Maderas Cerámicas. *Boletín de la Sociedad Española de Cerámica y Vidrio* 2002, **41**, 377–384.
15. Sieber, H., Friedrich, H., Kaindl, A. and Greil, P., Crystallization of SiC on biological carbon precoursers, bioceramics: materials and applications III. In *Ceramics Transactions, Vol 110*. The American Ceramic Society, 2000, pp. 81–92.
16. Sieber, H., Vogli, E. and Greil, P., Biomorphic SiC-ceramic manufactured by gas phase infiltration of pine wood. In *Ceramic Engineering and Science Proceedings, Vol 22*, 2001, pp. 109–116 [4, 25th Annual Conference on Composites, Advanced Ceramics, Materials, and Structures: B, 2001].
17. Vogli, E., Sieber, H. and Greil, P., Biomorphic SiC-ceramics prepared by Si-vapor phase infiltration of wood. *J. Eur. Ceram. Soc.* 2002, **22**, 2663–2668.
18. Vogli, E., Mukerji, J., Hoffmann, C., Kladny, R., Sieber, H. and Greil, P., Conversion of oak to cellular silicon carbide by gas-phase reaction with silicon monoxide. *J. Am. Ceram. Soc.* 2001, **86**(6), 1236–1240.
19. Sieber, H., Friedrich, H., Zeschky, J. and Greil, P., Lightweight ceramic composites from laminated paper structures. In *Ceramic Engineering and Science Proceedings, Vol 21*, 2000, pp. 129–134 [4, 24th Annual Conference on Composites, Advanced Ceramics, Materials, and Structures: B, 2000].
20. Sugiyama, K. and Kishida, T., Pressure-pulsed chemical vapor infiltration of SiC to porous carbon from a gas system SiCl4/H2. *J. Mater. Sci.* 1996, **31**, 3661–3665.
21. Ohzawa, Y., Hoshino, H., Fujikama, M., Nakane, K. and Sugiyama, K., Preparation of high temperature filter by pressure-pulsed chemical vapor infiltration of SiC into carbonized paper-fibre preforms. *J. Mater. Sci.* 1998, **33**, 5259–5264.
22. Ohzawa, Y., Sadanaka, A. and Sugiyama, K., Preparation of gas-permeable SiC shape by pressure-pulsed chemical vapor infiltration into carbonized cotton cloth preforms. *J. Mater. Sci.* 1998, **33**, 1211–1216.
23. Ohzawa, Y., Nakane, K., Gupta, V. and Nakajima, T., Preparation of SiC based cellular substrate by pressure-pulsed chemical vapor infiltration into honeycomb-shaped paper preforms. *J. Mater. Sci.* 2002, **37**, 2413–2419.
24. Webb, P. A. and Orr, C., *Analytical Methods in Fine Particle Technology*. Micromeritics Instrument Coporation, USA, 1997.

25. *DIN Norm 52 292 Teil 1*, Bestimmung der Bruchfestigkeit: Doppelring-Biegeversuch an plattenförmigen Proben mit kleinen Prüfflächen, DK 666.151:620.174, April, 1984.
26. Popovska, N., Almeida Streitwieser, D., Gerhard, H. and Emig, G., Kinetic analysis of the low temperature CVD of silicon/silicon carbide from methyltrichlorosilane/hydrogen for the ceramization of biomorphic carbon preforms. In *Proceedings of the International Symposium on Chemical Vapor Deposition XVI and EUROCVD 14*, *Vol 1*, 2003, pp. 573–580.
27. West, A. R., Solid State Chemistry and Its Applications. John Wiley & Sons, Chichester, 1987, pp. 4–46 [reprint].
28. Kanino, T., Yaguschi, T. and Saka, H., In situ study of chemical reaction between silicon and graphite at 1400 °C in a high resolution/analytical electron microscope. *J. Electron Microsc*. 1994, **43**(2), 104–110.
29. Cimalla, V., Wöhner, Th. and Pezoldt, J., The diffusion coefficient of Si in thin SiC layers as a criterion for the quality of the grown layers. *Mater. Sci. Forum* 2000, **338–342**, 321–324.